Available free online at www.medjchem.com

Mediterranean Journal of Chemistry

Mediterranean Journal of Chemistry **2019**, 8(1), 30-41

Electrochemical deposition of Zinc on mild steel

Asmae El Fazazi, Moussa Ouakki * and Mohamed Cherkaoui

Laboratory of Materials Engineering and Environment (LMEE), Faculty of Sciences, University Ibn Tofail, BP 133, 14 000 Kenitra, Morocco

Abstract: Zn coating electrodeposited on a mild steel substrate in an acid bath was investigated using cyclic voltammetric and chronopotentiometry techniques. The effect of the current density on the deposition potential, the thickness of the deposit, deposition rate and current efficiency was investigated. The chemical composition and surface morphology of Zn coatings are characterized using Energy Dispersive X-Ray (EDX) spectrometer and Scanning Electron Microscopy (SEM), respectively. SEM observations indicated that the morphology of the film surface was modified from dense and uniaxial to disperse and dendritic with increasing the current density. The EDX analyses revealed the presence of Zn and O in the deposit.

Keywords: Zinc electrodeposition; cyclic voltammetry; current density; SEM; EDX.

Introduction

There are many technological processes to elaborate metallic thin films. Electrodeposition is the most commonly used one due to technical and environmental advantages. The electrochemical deposition method has some considerable benefits such as low-cost, convenience and allows for controlling of multiple experimental parameters. Improved performance of the electrodeposited coatings mainly depends on the controlled deposition parameters, such as temperature, pH value, electrolyte composition, potential, current density, concentrations of ions, the use of additives and stirring. Zn coatings are widely used in industry, not only because Zn is anodic to steel and thus sacrificially protects the base metals but also owing to its low cost and natural abundance. The deposition of Zn coatings usually relies upon the electrodeposition technique in an acidic or alkaline medium[1, 2].

Zn coatings are extensively electrodeposited from acidic electrolytes. Thus, a simple electrolyte bath was developed by Sriraman et al. [3] containing KCl as carrier electrolyte (The function of KCl is to increase the electrical conductivity and reduce the viscosity of the bath) [4], and H_3BO_3 as a buffer, which exhibits good results to inhibit ~~both~~ hydrogen formation by acting as a buffer and/or adsorbing at the electrode surface to block then the active centers [5-7].

The present work aims to investigate Zn electrodeposition from a simple free additives bath on mild steel. The electrochemical process was examined by cyclic voltammetry (CV) and chronopotentiometry. The effect of plating current density on the chemical composition and the surface morphology of Zn coatings has been investigated, and the deposits were characterized by analyzing their morphology and composition using Scanning Electron Microscopy (SEM) and Energy Dispersive X-Ray (EDX), respectively.

Experimental details

The electrochemical measurements were carried out using Potentiostat/Galvanostat/Voltalab PGZ 100 monitored by a computer (Voltamaster 4 Software). The voltammetric measurements were performed in the potential range between −0.3 V and −2 V [5].

A three-electrode electrochemical cell was employed with a working electrode of steel plate, having a surface area of 1 cm^2, a Pt counter electrode placed in a separate compartment and an Ag/AgCl/KCl saturated reference electrode.

Plates of E24 steel with a nominal chemical composition of 99.732%wt Fe, 0.17%wt C, 0.045%wt P, 0.045%wt Sand 0.008%wt N were used as the substrate. Before Zn plating, the substrates were mechanically

they are prepared using abrasive emery papers down to 2000 grit, decreased in ethanol at room temperature and finally rinsed with distilled water and immediately transferred to the electroplating bath.

The baths compositions are presented in Table 1. Analytical grade chemicals and distilled water were used for the preparation of the electrolyte. The pH was adjusted at 4.5 by adding 1 M HCl or 1 M NaOH

*Corresponding author: Moussa Ouakki
Email address: moussassaw@gmail.com
DOI: http://dx.doi.org/10.13171/mjc8119021318mo

Received November 3, 2018
Accepted November 22, 2018
Published February 13, 2019

solutions, and the temperature is set at ambient temperature 20 ± 1 °C. A current density of either 16 mA.cm^{-2}, 24 mA.cm^{-2}, 32 mA.cm^{-2} or 40 mA.cm^{-2} was applied for 20 min.

The electrodeposited surface morphologies of the coated samples, along with the chemical composition were examined using a Scanning Electron Microscopy (Quanta FEG 450) coupled with Energy Dispersive X-Ray (EDX) spectrometer and fulfilled in UATRS-CNRST-Rabat.

Table 1. Baths composition.

Electrolytes	$ZnSO_4,7H_2O$ (g.l^{-1})	H_3BO_3 (g.l^{-1})	KCl (g.l^{-1})
1	-	-	93.2
2	-	24.8	93.2
3	64.6	24.8	93.2

Results and Discussion

Electrochemical study

Fig.1 shows the voltammogram realized in electrolyte 1. We note that the current density is fully stable between -0.3 V and -1.3 V vs. Ag/AgCl. No current was observed until the potential reaches values higher than -1.3 V, then, the cathodic current begins to increase rapidly, which is associated with hydrogen reduction according to [7]:

$$2H_2O + 2e^- \rightarrow H_2 + 2OH^-$$

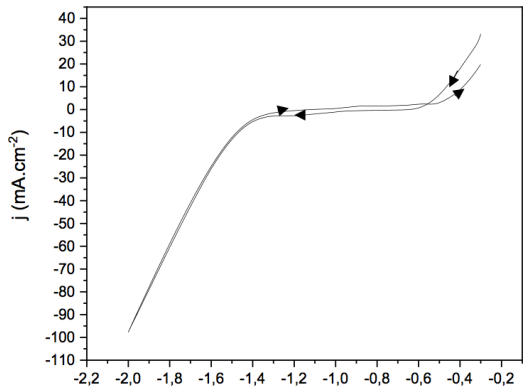

Figure 1. Cyclic voltammogram on a Fe substrate in KCl solution at pH = 4.5 (electrolyte 1), scan rate = 25 mV/s.

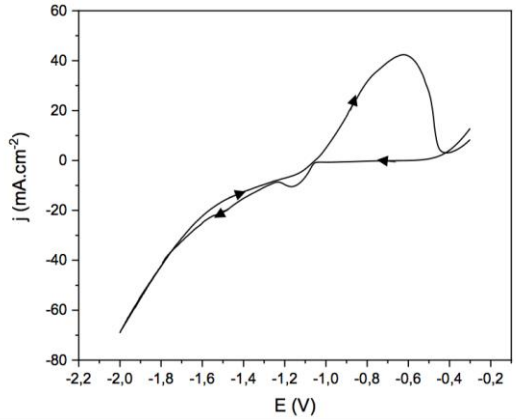

Figure 3. Cyclic voltammogram of mild steel in an electrolytic bath containing Zn(II), scan rate = 25 mV/s.

The voltammogram realized in a solution containing KCl+H_3BO_3 (Fig.2) has the same shape as in electrolyte 1. Boric acid is considered a very weak acid, with a tabulated ionization constant around pK_a= 9.2 [8]. Yet, in the presence of a strong base like NaOH (pKa =14.8), a reaction takes place according to the following equation:

$$H_3BO_3 + NaOH \rightarrow H_2BO_3^- + Na^+ + H_2O$$

Therefore, boric acid does not have any effect on the hydrogen evolution reaction.

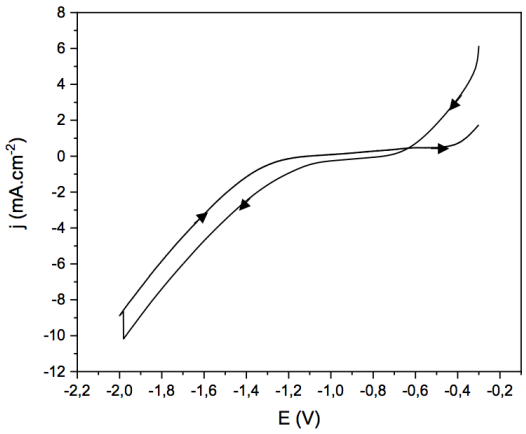

Figure 2. Cyclic voltammogram of a Fe substrate in KCl+H_3BO_3 solution at pH = 4.5 (electrolyte 2), scan rate = 25 mV/s.

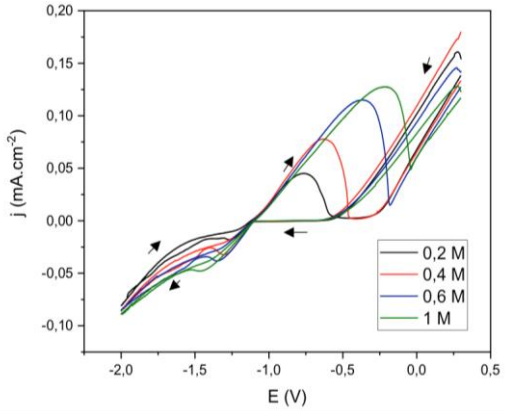

Figure 4. Cyclic voltammograms performed on mild steel from an electrolytic bath containing different Zn concentrations

In Fig.3, the cathodic current increases sharply at -1.05 V vs. Ag/AgCl and gives rise to a cathodic peak at around -1.17 V vs. Ag/AgCl. This peak is related to Zn^{2+} reduction during the cathodic scan according to the following reactions [9]:

$$Zn^{2+} \rightarrow {Zn^{2+}}_{ads}$$
$${Zn^{2+}}_{ads} + e^{-} \rightarrow {Zn^{+}}_{ads}$$
$${Zn^{+}}_{ads} + e^{-} \rightarrow Zn$$

At about -1.55V, we perceive an inflexion point; it is probably due to the formation of zinc in preference to hydrogen. In fact, with increasing current density. Zinc displaces hydrogen already on the surface, preventing the thermodynamically favored hydrogen reaction [9].

When the potential scan is reversed, a hysteresis appears. Probably this is a crossover potential at which nucleation and growth take place [1-10]. During the reverse anodic scan, an oxidation peak appears, at -0.6 V, which represents the anodic dissolution of the previously deposited zinc metal.

Effect of Zn concentration

Voltammetric study

The effect of Zn concentration, in the range 0.2 to 1 M, on the cyclic voltammograms is shown in Fig.4. Cyclic voltammograms of Zn reduction show that increasing the Zn concentration causes a gradual increase in cathodic current. Additionally, as the Zn concentration is increased, the area covered by the anodic curve is increased, indicating that much more zinc is deposited. This can be connected with the increase in Zn deposition efficiency during the cathodic process with an increase in solution Zn concentration [11].

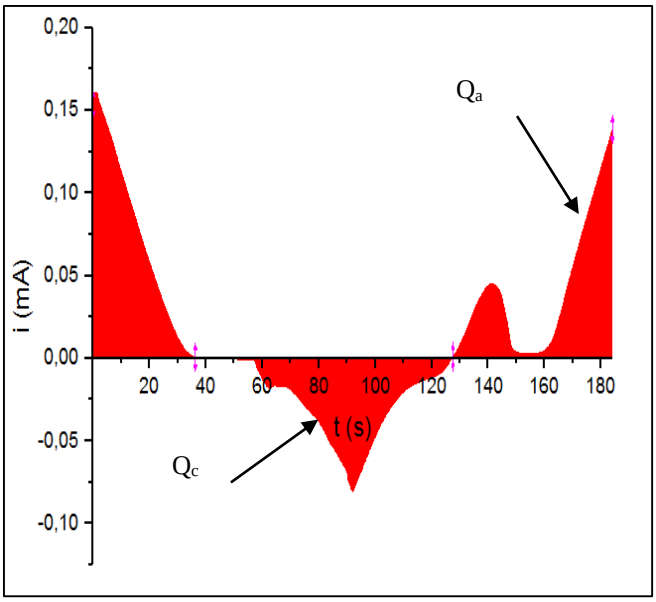

Figure 5. The voltammogram i=f(E) converted into i=f(t)

Electric charge

The effect of Zn concentration on the electric charge has been studied. To calculate the cathodic charge Q_c, related to Zn deposition and the anodic charge Q_a, related to Zn dissolution, we have integrated the areas of reduction and oxidation peaks of Zn voltammograms **(**Fig. 5**)**. The evolution of the cathodic and anodic charges as a function of Zn concentration is shown in Fig. 6.

We note that Q_c decreases while Q_a increases with increasing Zn concentration. The improvement in Q_a variation can be attributed to the enhancement of the kinetic of Zn deposition with increasing Zn concentration as well as the metal oxidation, while the weaker value of Q_c indicates that the discharge of H^+ protons becomes more difficult with increasing the Zn concentration [12, 13].

Current efficiency

The current efficiency of Zn deposition is calculated owing to the ratio of the charge of dissolution Q_a to the charge of deposition Q_c during Zn electrodeposition with different Zn concentrations. The current efficiency CE is calculated according to the following equation [9]:

$$CE(\%) = \frac{Q_a}{Q_c} \times 100$$

One notices that for a Zn concentration more than 0.4M, the current efficiency exceeds 100%, it is probably due to the formation of a film of zincate as a result of zinc dissolution, i.e. a dissolution/precipitation process occurs, according to [14]:

$$Zn(SO)_4 + 2NaOH \rightarrow Zn(OH)_2 + Na_2SO_4$$
$$Zn(OH)_2 + 2NaOH \rightarrow Na_2ZnO_2 + 2H_2O$$
$$Zn(SO)_4 + 4NaOH \rightarrow Na_2ZnO_2 + Na_2SO_4 + 2H_2O$$

The dissolution of the oxidation product (as$Zn(OH)_2)^-$) is characterized by the ratio, $\frac{Q_a}{Q_c}$ of the charges under the anodic, and corresponding cathodic peak. When a dissolution process accompanies metal oxidation with oxide film formation, the anodic/cathodic charge ratio $\frac{Q_a}{Q_c}$ is usually >1 and mass-transport dependent [13] **(**Fig.7**).**

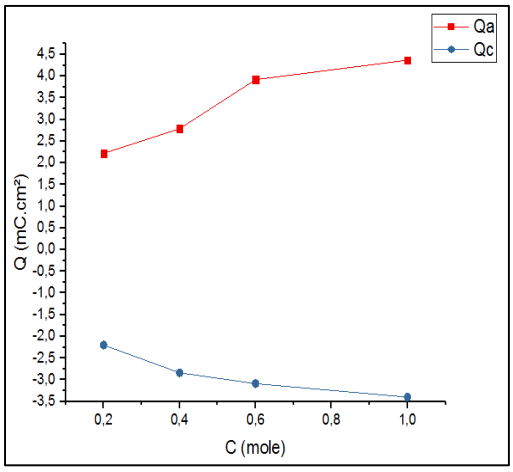

Figure 6. The evolution of Q_c and Q_a as a function of Zn concentration

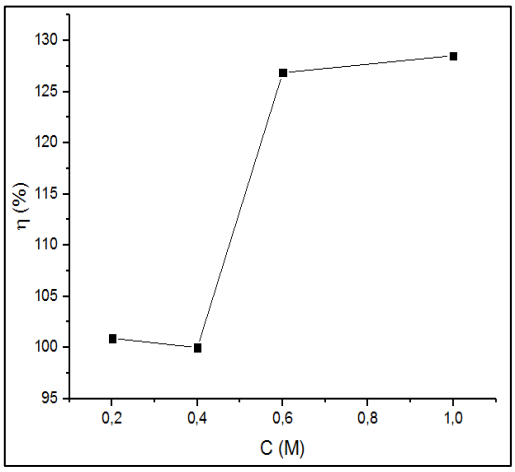

Figure 7. Current efficiency variation as a function of Zn concentration

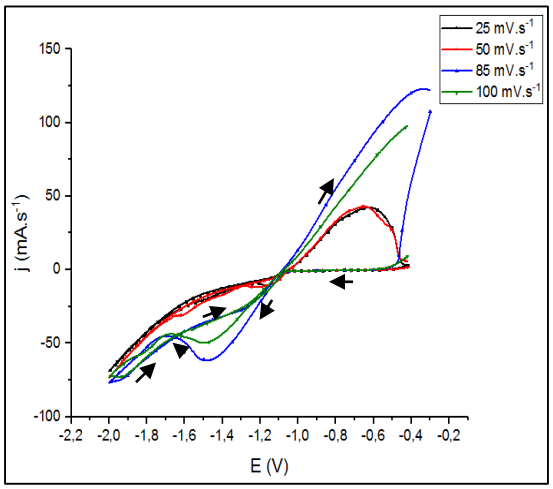

Figure 8. The voltammograms of Zn deposition/dissolution on mild steel at various scan rates

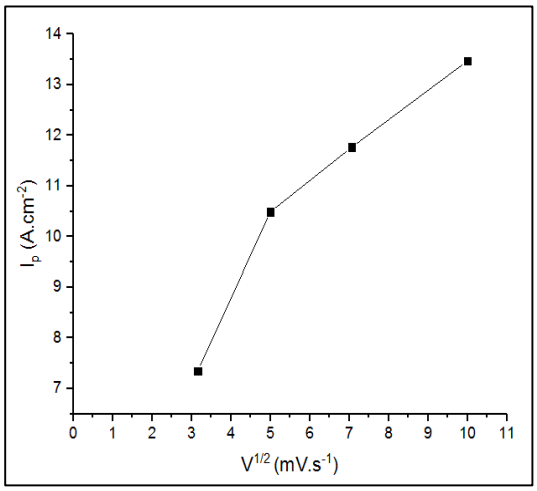

Figure 9. The evolution of the intensity of the peak I_p as a function of the square root of the scan rate v^1

Effect of scan rate

Voltammetric study

Fig.8 shows the voltammograms of Zn deposition on mild steel at various scan rates. The anodic peak potentials became more positive with the scan rate while the cathodic peak potentials became more negative, indicating that reduction becomes more difficult and the system is irreversible [15].

The study of the evolution of the intensity of the peak I_p as a function of the square root of the scan rate $v^{1/2}$can inform us about the nature of the limiting step in an electrochemical process. The peak current density, for an irreversible voltammogram, is given by the following equation [16]:

$$I_p = 0.4958\frac{(nF)^{3/2} \propto^{1/2}}{(RT)^{1/2}} SD^{1/2}v^{1/2}C^{sol}$$

Where: n : the valency number of ions of the substance, F (C.mol^{-1}): the Faraday constant (96500), α: the anodic charge transfer coefficient (0<α<1), R (J·mol^{-1}·K^{-1}): the gas constant (8.314462), S (cm^2): the electrode area, D (m^2.s^{-1}): the diffusion coefficient of electro-active species and C^{sol} (mol.cm^{-3}): the concentration of electro-active species in the solution.

The plot (Fig.9) is a slight concavity curve facing scan rates; this means that the zinc reduction process is associated with charge transfer coupled with mass transfer.

The evolution of the potential of the peak Ep as a function of the natural logarithm of the scan rate $ln(v_b)$ given by the following formula [16], (where k^0(cm.s^{-1}) is a rate constant):

$$E_p = E^{0\prime} - \frac{RT}{\propto nF}[0.780 + \ln\left(\frac{D^{1/2}}{k^0}\right) + \ln\left(\frac{\propto nFv}{RT}\right)^{1/2}]$$

Allows the characterization of the reaction mechanism on the electrode. Since, $E_p = f(ln(v_b))$ is a line with a slope different from zero, thus the reaction to the electrode is slow (Fig.10) [17].

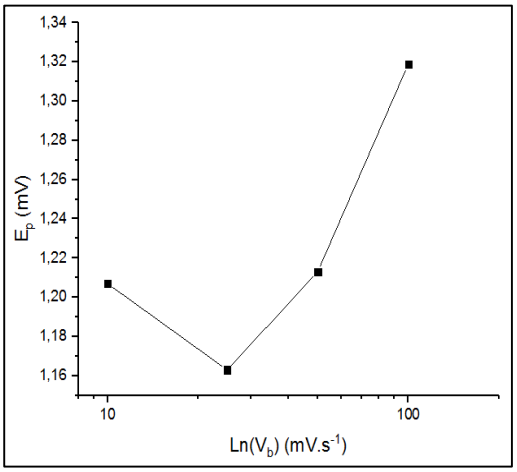

Figure 10. The evolution of the potential of the peak E_p as a function of the natural logarithm of the scan rate ln(v_p)

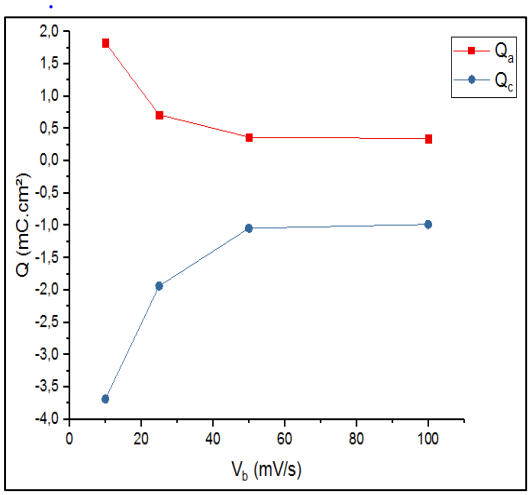

Figure 11. The evolution of Q_c and Q_a as a function of the scan rate

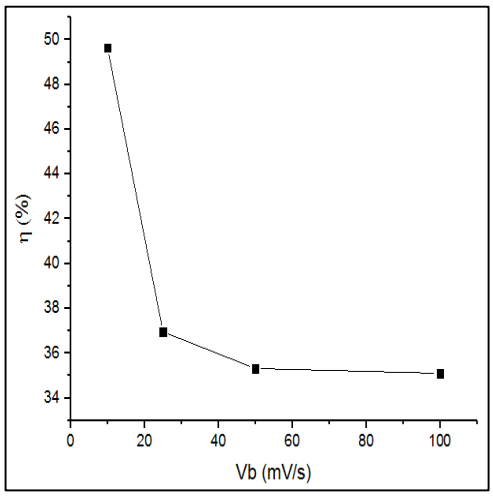

Figure 12. Current efficiency variation as a function of scan rate

Electric charge

We note that Qc increases, with increasing the scan rate, showing that a big part of the cathodic charge is consumed in hydrogen evolution, while Qa decreases, which can be attributed to the decrease of the kinetic of Zn deposition, with the rise of the scan rate [12] (Fig.11).

Current efficiency

In Fig.12, we can quantify the contribution of the hydrogen evolution during Zn electrodeposition with different scan rates. The current efficiency decreases gradually from 49.72% to 35.85% with increasing the scan rate from 10 mV.s^{-1} to 100 mV.s^{-1}. Probably this is because at slow scan rates, Zn is correctly reduced on the surface, whereas, at faster scan rates, the species formed remain into the bulk electrolyte because they do not have enough time to be reduced [18]

Galvanostatic deposition

Effect of current density in the plating bath on deposition potential, thickness, deposition rate and current efficiency

Electrodeposition can be performed by controlling either the potential or current. In industrial coatings preparation, the current step method, also known as the galvanostatic method, is the most practical. The advantage of the galvanostatic method is that the thickness of the as-deposited layer can be easily controlled according to Faraday's law [5]. Accordingly, the deposition of a Zn coating can be applied using different current densities. However, the applied current densities should be superior to the limiting current density of Zn deposition, which is ≈ -10 mA.cm^{-2} as can be seen in Zn voltammogram exposed above (Fig. 3). Galvanostatic experiments were carried out in a range of current density varying from 16 to 40 mA.cm^{-2}.

Fig.13 presents the variation of the deposition potential (Ed) during Zn electrodeposition with different current densities. A further increase in current density leads to a notable shift of Ed towards more negative values. For instance, Zn deposition at 16 mA.cm^{-2}, 24 mA.cm^{-2}, 32 mA.cm^{-2} and 40 mA.cm^{-2} exhibit an average deposition potential E_d of -1.42 V, -1.51 V, -1.62 V and -1.85 V respectively. Further increase of the current density leads to stronger potential oscillations in the curves due to intensive hydrogen evolution [19, 20].

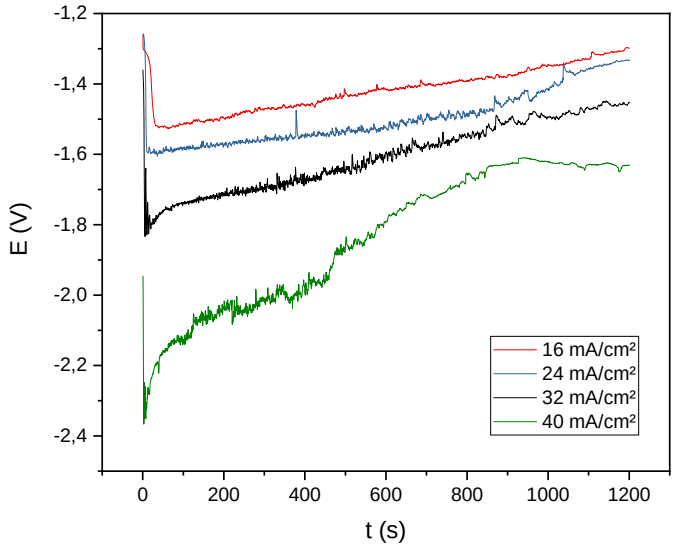

Figure 13. The evolution of the deposition potential E_d during Zn electrodeposition with different current densities

The effect of current density on the thickness(e), which is given by the following relation:

$$e = \frac{\Delta m}{\rho S}$$

Where Δm (g): the deposited mass of coating; ρ (g.cm^{-3}): the density of coating and S (cm²): the surface area of the substrate, is shown in **Table 2**. It can be seen that the thickness increases with increasing current density, as well as the deposition rate υ (µm.h^{-1}), which is calculated according to the following equation:

$$\upsilon = \frac{m_2 - m_1}{\rho S t}$$

Where m_2 (g): mass of the sample after the deposition, m_1 (g): mass of the sample before the deposition and t (s): deposition time.

Table 2. Effect of current density on thickness, deposition rate and current efficiency

Current density (j) mA.cm^{-2}	Thickness (e) µm	Deposition rate (υ) µm.h^{-1}	Current Efficiency (CE) %
16	5.7	17.1	63
24	6.4	19.2	47
32	8.8	26.4	46.56
40	11.7	35.1	52.5

Moreover, it is observed (Table 2) that the current efficiency (CE) decreases with increasing current density that could be attributed to the rapid increase in hydrogen evolution. The CE is obtained using the equation:

$$CE = \frac{\Delta m}{m_{th}} * 100$$

m_{th} is calculated by the mean of Faraday's law:

$$m_{th} = \frac{jtM}{nF}$$

Where j (mA.cm^{-2}): the applied current density and M (g.mol^{-1}): molar mass of the substance.

Since in electrodeposition processes hydrogen is the second element produced at the cathode, many works had investigated the influence of hydrogen evolution on the reaction of zinc deposition [19-22] and depending on the composition of the electrolyte and plating conditions; the current efficiency may vary over a broad range. For the evaluation of the impact of hydrogen evolution reaction (HER) on the current efficiency, Dundlker et al. [23] have approximated the current efficiency (CE) by the ratio of the zinc reaction current density to the total electrode current density by the following equation:

$$CE \approx \eta_j = \frac{j_{Zn}}{j}$$

Where j_{Zn} is the current density of zinc reaction and j is the total electrode current density. Considering:

$$j = j_{Zn} + j_{H_2}$$

Where j_{H_2} is the current density of hydrogen reaction. Fig. 14 shows the variation of the polarization of Zn electrode, in case of considering the effect of HER (j_x ; $x = Zn\ or\ H_2$) and in case of neglecting its effect ($j_{x\backslash H_2}$), with different current densities.

By neglecting HER effect, we note that zinc reaction is under mass transfer limitation, which is exhibited by the presence of the plateau of the zinc limiting current density. Nevertheless, taking in consideration the HER effect on the zinc reaction, we distinguish a significant run of the HER near the mass transfer limitation of the zinc deposition, indicating the improvement of the mass transfer rate of the zincate ions with hydrogen evolution [23].

Fig. 15 shows the variation of the CE as a function of current density. The drop in the CE with increasing the current density is attributed to the HER. However, with higher current densities, the displacement of hydrogen ions by zinc leads to an increase of current efficiency. The rising hydrogen bubbles may cause extra convection within a diffusion layer, leading to enhanced mass transport of zincate ions to an electrode surface, which partially compensates the drop of the current efficiency of the zinc deposition at higher current flows [23].

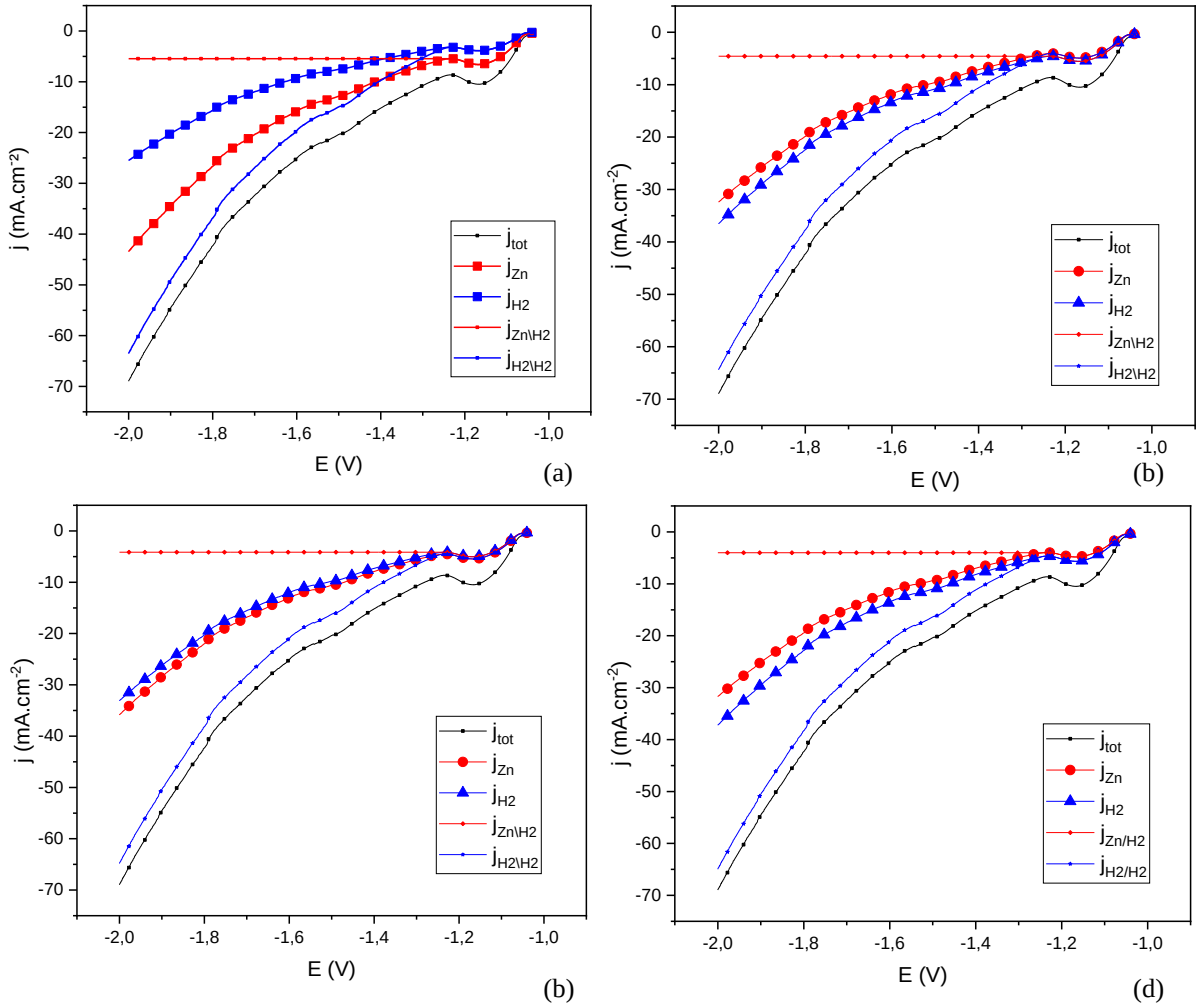

Figure 14. The variation of the polarization of Zn electrode, in case of considering the effect of HER (j_x ; x = Zn or H_2) and in case of neglecting its effect ($j_{x\backslash H_2}$), with different current densities: (a) 16 mA.cm^{-2}, (b) 24 mA.cm^{-2}, (c) 32 mA.cm^{-2} and (d) 40 mA.cm^{-2}

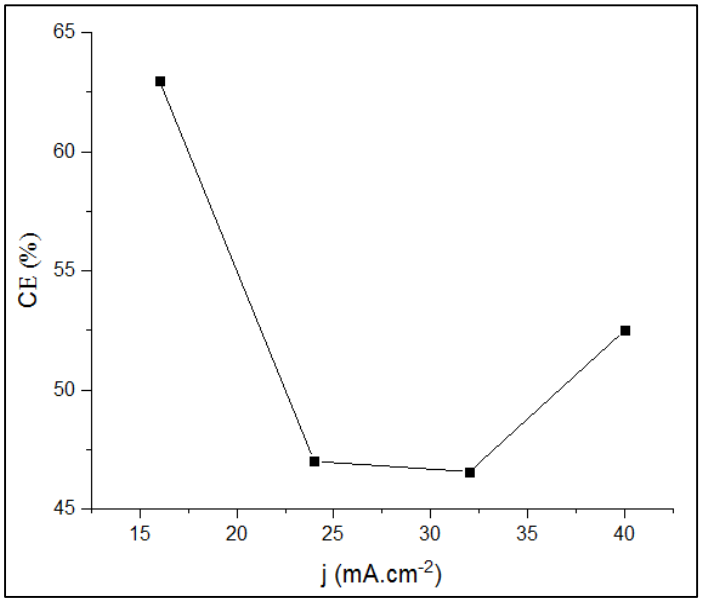

Figure 15. The variation of the CE as a function of current density

Effect of the applied current density on the morphology and crystallographic structure of Zn coating

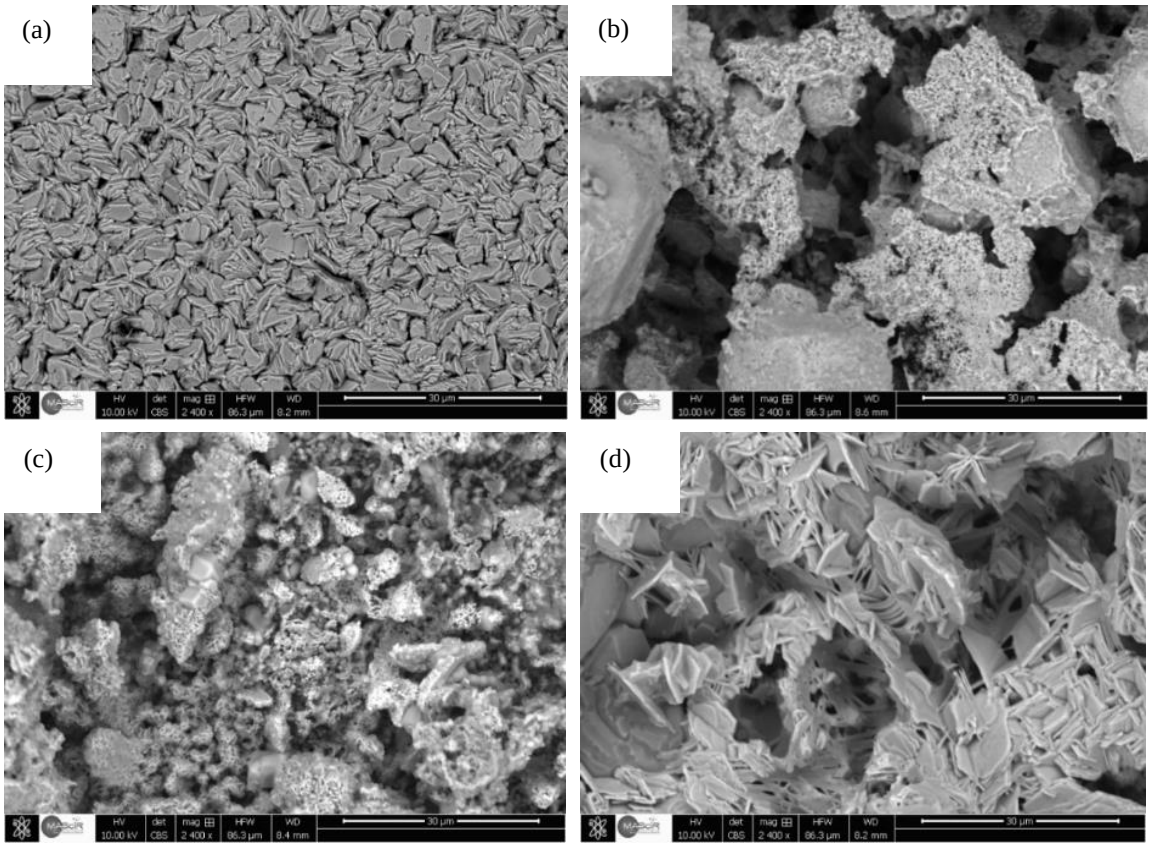

Figure 16. SEM images of Zn deposit obtained with different current densities: (a) 16 mA.cm^{-2}, (b) 24 mA.cm^{-2}, (c) 32 mA.cm^{-2} and (d) 40 mA.cm^{-2}

Morphological characterization

SEM images of investigated Zn coatings are presented in Fig. 16a-d. At a low current density **(**Fig. 16a), a platelet morphology is observed; the grains have typical hexagonal close-packed crystals, which is a typical morphology of Zn deposits in the absence of additives. The deposit is compact, showing a homogeneous structure which affords a smooth and

brilliant aspect. With increasing the current density **(**Fig. 16b-c**)**, coarse grains, porous and blackish grey deposits are obtained. With higher current density (40 mA.cm^{-2}) a flower-like shape is observed (Fig. 16d), with a transient from bidimensional to the tridimensional structure. However, the heterogeneous structure and the random growing of the nano-grains provides a dull and rough deposit [2, 11, 17, 24-28]. This result is by those reported by N. Alias et al. [29], who explained that the change in morphology of Zn deposit from dense and uniaxial to disperse and dendritic was due to the increase in current density used for the deposition.

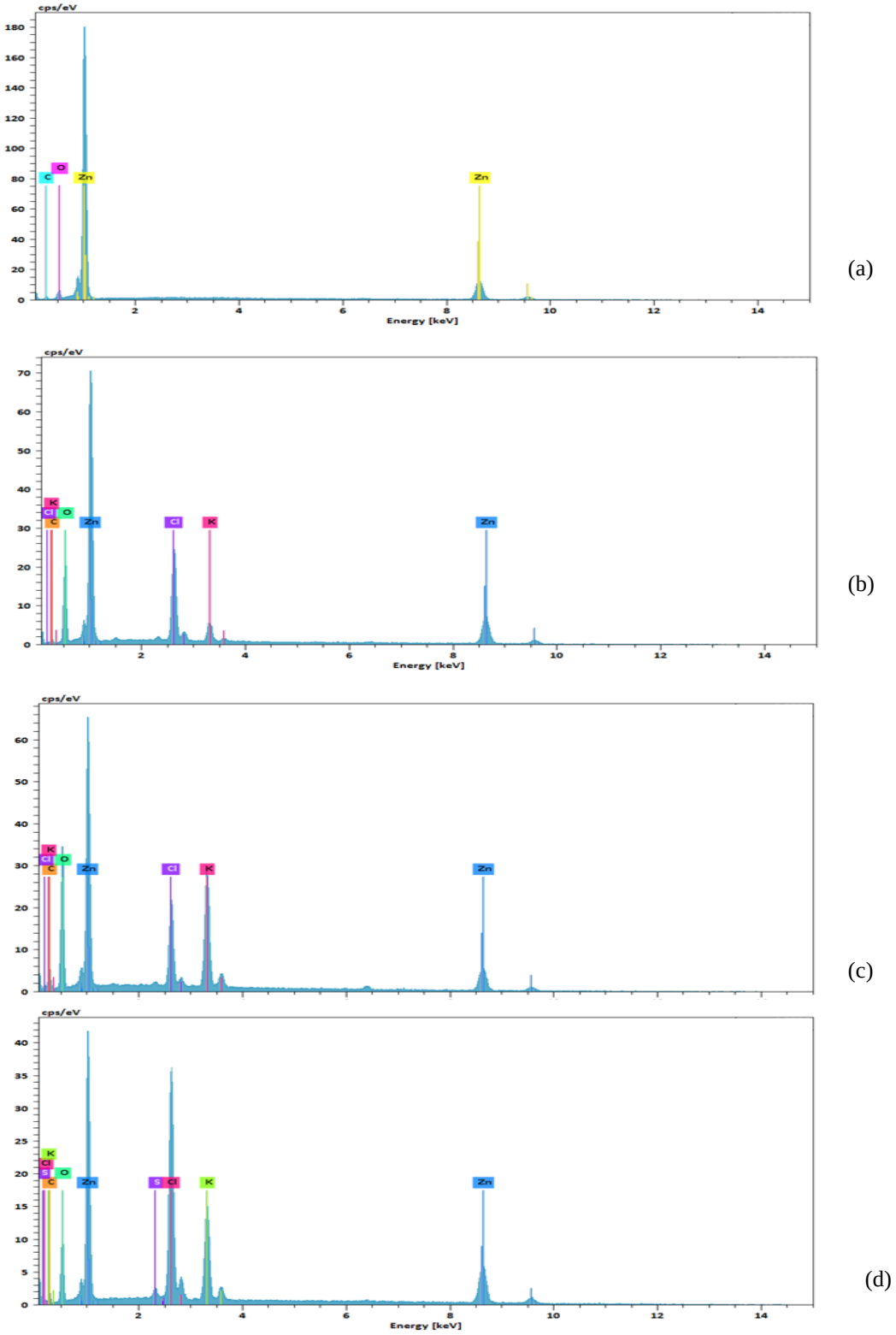

Figure 17. EDS analysis of the Zn coating obtained with different current densities: (a) 16 mA.cm^{-2}, (b) 24 mA.cm^{-2}, (c) 32 mA.cm^{-2} and (d) 40 mA.cm^{-2}

Compositional analysis (EDS)

The EDS analysis shows the elemental composition of Zn deposit on a steel substrate. The spectrum for a deposition at low current density shows a prominent peak of Zn, and noteworthy peaks of O and C **(**Fig. 17a**)**. The element of carbon mainly comes from the steel substrate, while the oxygen should result from some oxides on the top surface. When we increase the current density, new peaks of K, Cl and even S appeared **(**Fig. 17b-c-d**)** [30-32]. Indeed, the rising hydrogen bubbles may cause extra convection within a diffusion layer, inducing K, Cl and S transport and adsorption on the deposit. Rogers et al. [33] reported that incorporation of sulfur increases with decreasing current density which is in disagreement with our results. Nitin et al. [34] suggest that sulfur (S) and carbon (C) adsorb the crystallographic surface before being incorporated in the coating.

The results of the chemical composition of the obtained coatings are presented in **Table. 3**. They exhibit the average value computed using four measurements.

Table 3. Chemical composition of the obtained deposit at different current densities.

Current density mA.cm^{-2}	**C %**	**O %**	**S %**	**Cl %**	**K %**	**Zn %**
16	15.81	11.26	_	_	_	72.92
24	8.55	38	_	14.1	3.25	35.6
32	9.02	34.03	1.02	7.31	11.66	36.95
40	6.50	15.42	7.52	21.88	24.35	24.31

Conclusion

In the present study, Zn coatings were produced by electrodeposition technique from a simple free additives bath on mild steel. The effect of the current density on the deposition potential, the thickness of the deposit, deposition rate and current efficiency was investigated, as well as the composition and the morphology of the elaborated deposits. The outcome of the results can be summarized as follows:

- Zn reduction is a slow reaction, which becomes more difficult with increasing the scan rate, because of HER, and is associated with charge transfer coupled with the mass transfer (diffusion).
- An increase in Zn concentration leads to an improvement in Zn deposition efficiency.
- A further increase in current density leads to a notable shift of Ed towards more negative values and an intensive hydrogen evolution.
- The thickness increases with increasing current density, while the current efficiency decreases. However, with higher current density, HER partially compensates the drop of the current efficiency, producing an enhancement in its value.
- The change in morphology of Zn deposit from dense and uniaxial to disperse and dendritic was due to the increase in current density.
- The EDX analyses revealed the presence of Zn and O.
- An optimum Zn electrodeposition is achieved using 0.4 M $ZnSO_4$, 0.4 M H_3BO_3, 1.25 M KCl and applying a current density of 16 mA.cm^{-2} for 20 min.

References

1- Ö. Rasim, H.K. Ismail and K. Orhan, A Study on the Electrodeposited Cu-Zn Alloy Thin Films. Metallurgical and materials transactions a, **2016**, 47A, 5609-5617.

2- Y. Yang, S. Liu, X. Yu, C. Huang, S. Chen, G. Chen and Q.H. Wu, Effect of additive on zinc electrodeposition in acidic bath, Surface Engineering, **2014**, 000, 1-6.

3- K.R. Sriraman, S. Brahimi, J.A. Szpunar, J.H. Osborne and S. Yue: Characterization of corrosion resistance of electrodeposited Zn-Ni Zn and Cd coatings, Electrochimica Acta, **2013**, 105, 314-323.

4- D.K. Sahoo, H. Singh and N. Krishnamurthy, Electrochemical deposition of La-Mg alloys in $LaCl_3$-$MgCl_2$- KCl system with molten salt electrolysis process, J. Min. Metall. Sect. B-Metall. **2014**, 50 (2) B, 109-114.

5- N. Loukil and M. Feki, Electrodeposition of Zn-Mn alloy coatings deposited from acidic chloride baths, Effect of deposition conditions on the Zn-Mn electroplating, morphological and structural characterization, Applied Surface Science, Applied Surface Science, **2017**, 410, 574-584, doi: 10.1016/j.apsusc.2017.02.075.

6- D. Sylla, J. Creus, C. Savall, O. Roggy, M. Gadouleau, Ph. Refait, Electrodeposition of Zn-Mn alloys on steel from acidic Zn-Mn chloride solutions, Thin Solid Films, **2003**, 424, 171-178

7- R. Tena-Zaera, J. Elias, G. Wang, and C. Levy-Clement, Role of Chloride Ions on Electrochemical Deposition of ZnO Nanowire Arrays from O2 Reduction, J. Phys. Chem.C, **2007**, 111, 16706- 16711.

8- M. Celeste C. Azevedo and Ana M.V. Cavaleiro, The Acid-Base Titration of a Very

Weak Acid: Boric Acid, Journal of chemical education, **2012**, 89, 767−770.
9- P.C. Foller, Improved slurry zinc/air systems as batteries for urban vehicle propulsion, Journal of applied electrochemistry, **1986**, 16, 527-543.
10- N.N. Che Isa, Y. Mohd, M. H. Mohd Zaki and S.A. Syed Mohamad, Characterization of Copper Coating Electrodeposited on Stainless Steel Substrate, International Journal of Electrochemical Science, **2017**, 12, 6010-6021, doi: 10.20964/2017.07.58.
11- A.E. Elsherie, Effects of cobalt, temperature and certain impurities upon cobalt electro-winning from sulfate solutions. Journal of Applied Electrochemistry, **2003**, 33, 43-49.
12- E.C. Pereira, J.S. Santos, R. Matos and F. Trivinho-Strixino, Effect of temperature on co-electrodeposition in the presence of boric acid, Electrochimica Acta, **2007**, 53, 644-649.
13- D. C. W. Kannangara and B. E. Conway, Zinc Oxidation and Redeposition Processesand Carbonate Solutions in Aqueous Alkali. J. Electrochem. Soc., Electrochemical Science and Technology, **1987**, 134, N°4, 894-905.
14- A. P. Chatterjee, P. Mitra and A. K. Mukhopadhyay, chemically deposited zinc oxide thin film gas sensor, Journal of materials science, **1999**, 34, 4225-4231
15- R. Sekar, S. Jayakrishnan and V. S. Muralidharan, Electrochemical behaviour of zinc acetate complexes: a cyclic voltammetry study, Transactions of the Institute of Metal Finishing, **2005**, 83, 300-302.
16- Trémillon B., Electrochimie analytique et réactions en solution-Tome 2 Réactions et méthodes électrochimiques; ed. By Masson: Paris, **1993**.
17- R.S. Nicholson and I. Shain, Single scan and cyclic methods applied to reversible, irreversible, and kinetic systems, Analytical Chemistry, **1964**, 36, 706-723.
18- T. Boiadjieva, M. Monev, A. Tomandl, H. Kronberger, and G. Fafilek, Electrochemical studies on Zn deposition and dissolution in sulphate electrolyte, Journal of Solid State Electrochemistry, **2009**, doi: 10.1007/s10008-008-0594-3.
19- T. Casanova, F. Soto, M. Eyraud and J. Crousier, Hydrogen absorption during zinc plating on steel, Corrosion Science, 1997,39, 529-537.
20- Tz. Boiadjieva-Scherzer, H. Kronberger, G. Fafilek and M. Monev, Hydrogen evolution reaction on electrodeposited Zn-Cr alloy coatings, Journal of Electroanalytical Chemistry, **2016**. doi: 10.1016/j.jelechem.2016.10.059.
21- M. Monev, L. Mirkova, I. Krastev, Hr. Tsvetkova and St. Rashkov, Effect of brighteners on hydrogen evolution during zinc electroplating from zincate electrolytes, Journal of applied electrochemistry, **1998**, 28, 1107-1112.
22- D. R. Gabe: The role of hydrogen in metal electrodeposition Processes. Journal of applied electrochemistry, **1997**, 27, 908-915.
23- J. Dundálek, I. Šnajdr, O. Libánský, J. Vrána, J. Pocedič, P. Mazúr, and J. Kosek: Zinc electrodeposition from flowing alkaline zincate solutions, Role of hydrogen evolution reaction. Journal of Power Sources, **2017**, 372, 221-226. doi: 10.1016/j.jpowsour.2017.10.077.
24- M. Froment and G. Maurin, Etude en microscopie électronique de la morphologie des dépôts électrolytiques de zinc, Electrodeposition and Surface Treatment, **1975**, 3, 245-260.
25- M. Kwon, D. Jo, S. H. Cho, H. T. Kim, J.-T. Park and J. M. Park: 'Characterization of the influence ofNi content on the corrosion resistance of electrodeposited Zn-Ni alloy coatings'. Surface & Coatings Technology, **2016**, 288, 163-170. doi: 10.1016/j.surfcoat.2016.01.027.
26- K. Raeissi, A. Saatchi, M.A. Golozar and J.A. Szpunar: Effect of surface preparation on zinc electrodeposited texture, Surface & Coatings Technology, 2005, 197, 229- 237. doi: 10.1016/j.surfcoat, **2004**.09.024.
27- P.K. Leung, C. Ponce-de-Leon, C.T.J. Low, and F.C. Walsh: 'Zinc deposition and dissolution in methanesulfonic acid onto a carbon composite electrode as the negative electrode reactions in a hybrid redox flow battery'. Electrochimica Acta, **2011**, 56, 6536- 6546. doi:10.1016/j.electacta.2011.04.111.
28- A. Gomes and M.I. da Silva Pereira, Pulsed electrodeposition of Zn in the presence of surfactants,.Electrochimica Acta, **2006**, 51, 1342-1350. doi:10.1016/j.electacta.**2005**.06.023.
29- N. Alias and A. A. Mohamad, Morphology study of electrodeposited zinc from zinc sulfate solutions as anode for zinc-air and zinc-carbon batteries, Journal of King Saud University - Engineering Sciences, **2015**, 27, 43-48. doi: 10.1016/j.jksues.2013.03.003
30- A. Sharma, Y. J. Jang and J. P. Jung: 'Effect of current density on the morphology of electroplated tin'. Surface Engineering, **2015**, 31, 458-464. doi: 10.1179/1743294414Y.0000000427.
31- K. Gang, L. Lingyan, L. Jintang, C. Chunshan and Z. Zheng: 'Study on lanthanum salt conversion coating modified with citric acid on hot dip galvanized steel'. Journal of rare earths, **2010**, 28, 461-465. doi: 10.1016/S1002-0721(09)60134-4.
32- J. Zhang, C. Gu and J. Tu, Potentiodynamic deposition and corrosion behavior of thin Zn-Sn coatings with layered structure and varied

composition from deep eutectic solvent'. Surface & Coatings Technology, **2016**, doi: 10.1016/j.surfcoat.2016.10.004

33- G. T. Rogers 1, M. J. Ware and R. Y. Fellows, The Incorporation of Sulfur in Electrodeposited Nickel, Using Thiourea as a Brightener and Leveler, Journal of the electrochemical society, 1960, 107, 677-682.

34- N. P.Wasekar, P. Haridoss, S.K. Seshadri, and G. Sundararajan: 'Influence of mode of electrodeposition, current density and saccharin on the microstructure and hardness of electrodeposited nanocrystalline nickel coatings'. Surface & Coatings Technology, **2016**, 291, 130-140. doi: 10.1016/j.surfcoat.2016.02.024.